# On-line estimation of $N$-qubit quantum state via continuous weak measurement and compressed sensing

**Sajede Harraz**[1], **Shuang Cong**[1] **and Kezhi Li**[2]

[1]Department of Automation, University of Science and Technology of China, Hefei 230027, P. R. China

[2]Imperial College London, London, SW7 2AZ, UK

E-mail: `scong@ustc.edu.cn`

October 2019

**Abstract.** In this paper, we propose an on-line state estimation method for an $N$-qubit quantum system based on the continuous weak measurement and compressed sensing. The quantum system is described by stochastic master equation. The continuous weak measurement operators for the $N$-qubit quantum system, which are indirectly acted on the quantum system, are derived according to the measurement operator results of two-level quantum system. The on-line time-varying measurement operators are obtained by means of the dynamic evolution equation of the system. The quantum state is on-line estimated by solving the optimization problem of minimizing the 2-norm with the positive definite constraints of density matrix, and we use the non-negative least squares algorithm to solve the optimization problem. Compressed sensing theory is used to reduce the number of the measurements in the process of on-line state estimation. In the numerical experiments, we study the effects of external control field, measurement rate and the different numbers of qubits on the performance in the proposed method. The minimum required number of measurements for 2, 3, 4 and 5 qubits are found. The fidelity accuracy of our proposed method can achieve more than 99% with small number of measurements.

## 1. Introduction

The fundemental task of reconstructing an unknown quantum state – known as quantum state tomography (QST), or quantum state estimation (QSE) – has been applied in quantum control, quantum computing and quantum information to characterize quantum states, such as trapped ions [1] and optical entangling gate [2]. In QST, the state of system is reconstructed based on the results of a collection of complete measurement set [3, 4, 5]. Specifically, standard QST reconstructs quantum states from a complete set of projective measurements with informationally complete observables obtained from separable ensembles[6, 7]. In recent years, other QST methods have been proposed using different measurements and technical approaches. For example, continuous weak measurement [8, 9, 10, 11] and sequential unsharp measurement [12] with estimation methods such as maximum likelihood and Baysian method [13, 14, 15] have been widely used in experiments [16, 17]. When the projective or strong measurements are acted, the state of the system will collapse to its eigenstates, thus one needs to reprepare the ensemble and measurement apparatus at each step [18]. The weak measurements offer a trade-off between information gain and the disturbance of the system [19]. Since weak measurement is not completely destructive, continuous measurements are applicable with weak measurements [20]. On-line quantum state estimation (OQSE) is a continuous state estimation at any moment by using continuous weak measurements with the help of some optimization algorithms [21, 22]. Its continues measuring process can make OQSE work together with the feedback control theory [23, 24]. When the system dynamics are known, one can produce continuous measurement operators in the Heisenberg picture [25, 26]. Most previous works on state estimation are off-line [27, 28], while in OQSE the state is estimated in real time as the system evolves dynamically [29, 30].

Compressed sensing (CS) is widely used for recovering sparse signals [31]. It focuses on matrices that can be approximated by low-rank matrices of rank $r \ll d$, where $d$ is the dimension of the signal. The CS theory can be efficiently applied in standard QST [32, 33] as well as real-time estimation [21, 34]. Without complete knowledge about the system, CS can reconstruct the state by making use of the optimization algorithm [35, 36]. In addition, this theory is robust to noise and continues to perform well when the measurements are imprecise or when the state can be approximated as a low-rank state [37]. Least square (LS) and compressed sensing are used for the estimation and solving the optimization problem by the prevalent convex optimization toolbox [21].

In this work, we propose a method of on-line state estimation for $N$-qubit system by means of continuous weak measurements and compressed sensing in real time. We completed the OQSE for one-qubit in our previous researches [29, 30]. The dynamic of the system is described by stochastic master equation in Schrodinger picture. The estimated state is reconstructed by solving a convex optimization problem with physical constraints. We verify the accuracy of the proposed estimation method by experimental simulations for 2, 3, 4 and 5-qubit systems. To evaluate the accuracy of the estimation we define fidelity and trace distance between actual state and estimated state. The influences of parameters: external control field, measurement rate and number of qubits are studied on the performance of the estimation by numerical simulations.

The paper's structure is as follows. In Sec. 1 we introduce the $N$-qubit quantum state on-line estimation and continuous measurement operators. In Sec. 2 numerical simulations and results analyses are given. Finally, the conclusion is given in Sec. 3.

## 2. On-line quantum state estimation (OQSE) setup

In general QSE setup, one needs to apply measurements and reconstruct the state density matrix of the system based on the results of the measurement. The measurement of a $d$-dimensional quantum state $\rho$ is measuring the expectation probabilities of $\rho$ projecting on different measurement operators. The expectation probability of $\rho$ projecting on the measurement operator $M_i$ is

$$\langle M_i(\rho)\rangle = Tr(\rho M_i) \tag{1}$$

where $M = \{M_1,\ M_2,\ ...,\ M_{d^2}\}$ is the set of complete measurement operators of $\rho$.

In QSE for an arbitrary quantum state $\rho$ with a $d * d$ density matrix, one needs at least $d^2 - 1$ mutually orthogonal measurement operators to accurately reconstruct $\rho$ as

$$\hat{\rho} = \frac{1}{d}\sum_{i=1}^{d^2} \langle M_i\rangle\, M_i \tag{2}$$

When the selected set of measurement operators is not complete, which implies that the measurement is informationally incomplete, the solution of $\rho$ in Eq. 2 is not unique and one cannot use Eq. 2 to reconstruct $\rho$. In this case, by considering compressed sending theory, the reconstruction problem of density matrix $\rho$ is transformed to the following optimization problem:

$$\min \|\hat{\rho}\|_* \ \ s.t.\ \ y = A.vec(\hat{\rho}) \tag{3}$$

where $\|\hat{\rho}\|_*$ is the nuclear-norm of $\hat{\rho}$, $vec(\cdot)$ represents the transformation from a matrix to a vector by stacking the matrix's columns in order on the top of one another; $A$ is the matrix form of all the sampled measurement operators $M_i$; and vector $y$ is the corresponding measurement values as Eq. 1.

### *2.1. Weak measurement operator design*

We design continuous weak measurement in presence of the dynamic evolution of the system. We make weak measurement in an ensemble system by coupling the ensemble to some probe which can be measured. At each instant time, the records of the expectation values corresponding to measurement operators by the indirect results of continuous weak measurements are obtained.

In this subsection we describe a model for measurement which consists of a measurement device called a probe $P$ and the coupling estimated system that is going to be measured, called system $S$. The measurement is the interaction between the probe and the system. One gets the information as the value of the system observable by reading off the probe.

The system $S$ has the Hamiltonian of $H_s$ and initial state of $|s\rangle$. The probe $P$ is a quantum device with Hamiltonian of $H_p$ and initial state of $|p\rangle$, with a complete, orthonormal set of basis states $|k\rangle$. Thus, the corresponding measurement operators of probe are $X = \sum I \otimes |k\rangle\langle k|$.

The probe $P$ and system $S$ are coupled and the initial state of the coupled system is $|\Psi\rangle = |s\rangle \otimes |p\rangle$, with the joint system Hamiltonian of $H = H_P \otimes H_S$. After the joint evolution of $S$ and $P$ for time $\Delta t$, the joint system state becomes $|\Psi(\Delta t)\rangle = U(\Delta t)|\Psi\rangle$, where $U(\Delta t) = \exp(-i\xi\Delta t H/\hbar)$ is the joint evolution operator , and $\xi$ represents the interaction strength between system $S$ and probe $P$. $|\Psi(\Delta t)\rangle$ is an entangled state composed of $S$ and $P$, which cannot be separately described with the states of $S$ and $P$.

At time $\Delta t$, a measurement is performed on the entangled state with the measurement operator $X = \sum I \otimes |k\rangle\langle k|$. This measurement is actually a projective measurement on $P$, and the outputs are the eigenvalues corresponding to $|k\rangle$. The state of the joint system after the weak measurement becomes

$$|\Psi_k(\Delta t)\rangle = (|k\rangle\langle k| \otimes I \bullet U(\Delta t)|p\rangle \otimes |s\rangle)/\Theta_k \tag{4}$$

where $\Theta_k = \sqrt{\langle\Psi(\Delta t)|\Pi_k|\Psi(\Delta t)\rangle}$.

After the projective measurement, the entanglement between $S$ and $P$ disappears, and the state of $S$ at time $\Delta t$ becomes $|s_k(\Delta t)\rangle$. The state of the joint system after the weak measurement can be represented as

$$|\Psi_k(\Delta t)\rangle = |k\rangle \otimes |s_k(\Delta t)\rangle \tag{5}$$

By substituting Eq. 5 into Eq. 4, we can obtain the state of the system after measurement as

$$|s_k(\Delta t)\rangle = \langle k| \otimes I \bullet U(\Delta t)|p\rangle \otimes |s\rangle/\Theta_k \tag{6}$$

The weak measurement operator $m_k$ is defined as

$$m_k = \langle k| \otimes I \cdot U(\Delta t) \cdot |p\rangle \otimes I \tag{7}$$

which is a Kraus operator and satisfies $\sum_k m_k^\dagger m_k = 1$. In this case, $\Theta_k$ becomes

$$\Theta_k = \sqrt{\langle s|{m_k}^\dagger m_k|s\rangle} \tag{8}$$

In such a way, we obtain the weak measurement operator $m_k$ in Eq. 7 on the system $S$.

Measurement operators in on-line state estimation are not a constant matrix group, but they are a set of time varying measurement operators $m_k(t)$. Here, we need to deduce the time varying measurement operators used in OQSE.

In the joint evolution operator $U(\Delta t) = \exp(-i\xi\Delta t H/\hbar)$, $\lambda = \xi\Delta t$ denotes the weak measurement strength, where $\hbar = 1$ and both the interaction strength $\xi$ and the evolution time $\Delta t$ are small values. When $\xi\Delta t \to 0$ the measurement is weak. The Taylor expansion of $U$ by neglecting more than three orders of magnitude is

$$U(\Delta t) \approx I \otimes I - i\xi\Delta t H - (\xi\Delta t)^2 H^2 \Big/ 2 \tag{9}$$

By replacing Eq.9 in Eq.7 we can obtain the expression of the weak measurement operator as

$$m_k(\Delta t) \approx I\,\langle k|\ p\rangle - i\xi\Delta t H_S\,\langle k|\ H_P\,|p\rangle - (\xi\Delta t)^2 H_S^2\,\langle k|\ H_P^2\,|p\rangle \Big/ 2 \tag{10}$$

Assume $r_k = (\xi\Delta t)H_S^2\,\langle k|\ H_P^2\,|p\rangle\,/2, k = 1, 2, ..., d$ , hence the general form of the weak measurement operator becomes:

$$m_k(\Delta t) = I\,\langle k|\ p\rangle - [r_k\lambda/2 + i\lambda H_S\,\langle k|\ H_P\,|p\rangle] \tag{11}$$

Suppose $\langle j \mid p \rangle = 1$ when $k = j$, we can obtain $m_j(t)$ as : $m_j(\Delta t) = I - (\xi r_{k=j}/2 + i\xi H_S)\Delta t$; and all the other measurement operators of $k \neq j$ can be combined as one operator as: $m_{k\neq j}(\Delta t) = m_{j\perp}(\Delta t) = \sqrt{r_{k\neq j}\Delta t}$, where $m_{j\perp}$ and $m_j$ are orthogonal and satisfy $(m_{j\perp})^2 + (m_j)^2 = I$. For the continuous weak measurements of a two-level quantum system, the measurement operator group contains two operators: $m_0(\Delta t)$ and $m_1(\Delta t)$. With a given operator $L$, the corresponding continuous weak measurement operators $m_0(\Delta t)$ and $m_1(\Delta t)$ can be constructed, respectively, as

$$\begin{aligned} m_0(\Delta t) &= m_j - i(1-\xi)H_S\Delta t \\ &= I - (\xi r_k/2 + iH(t))\,\Delta t \\ &= I - \left(L^\dagger L\big/2 + iH(t)\right)\Delta t \\ m_1(\Delta t) &= m_{k\neq j} = L\cdot\sqrt{\Delta t} \end{aligned} \tag{12}$$

where $L^\dagger L = \xi r_k$.

For $N$-qubit system, one needs $2^N$ measurement operators, which can be calculated by tensor products of $m_0$ and $m_1$ given in Eq. 12.

$$\begin{aligned} M_0(\Delta t) &= \underbrace{m_0(\Delta t)\otimes\ldots\otimes m_0(\Delta t)\otimes m_0(\Delta t)}_{N} \\ M_1(\Delta t) &= \underbrace{m_0(\Delta t)\otimes\ldots\otimes m_0(\Delta t)\otimes m_1(\Delta t)}_{N} \\ &\vdots \qquad\qquad \vdots \\ M_{2^N-1}(\Delta t) &= \underbrace{m_1(\Delta t)\otimes\ldots\otimes m_1(\Delta t)\otimes m_1(\Delta t)}_{N} \end{aligned} \tag{13}$$

where $\sum_{j=0}^{2^N-1} M_j(\Delta t) = 1$.

### *2.2. Dynamical model of the system*

The dynamic model of open quantum system is presented by stochastic master equation in Schrodinger picture as [38]

$$\begin{gathered} \rho(t+\Delta t) - \rho(t) = -\tfrac{i}{\hbar}[H(t),\rho(t)]dt + \sum\left[L\rho(t)L^\dagger - \left(\tfrac{1}{2}L^\dagger L\rho(t) + \tfrac{1}{2}\rho(t)L^\dagger L\right)\right]dt \\ +\sqrt{\eta}\sum\left[L\rho(t) + \rho(t)L^\dagger\right]dw\,,\ \ \rho_0 = \rho(0) \end{gathered} \tag{14}$$

where $\rho(t)$ is the density matrix of the system; $H(t)$ is the total Hamiltonian of the system which is $H(t) = H_S + H_P$; $H_S$ is the measured system Hamiltonian and $H_P$ the Hamiltonian of the probe system. Let $D[L,\rho] = L\rho L^\dagger - (1/2)\left(L^\dagger L\rho + \rho L^\dagger L\right)$, which is the decoherence effect of the measurement process, and a drift term expressed as a Lindblad form; $H[L,\rho] = L\rho + \rho L^\dagger$, is the stochastic diffusion term introduced by the measurement process expressed as a disturbance to the state of the quantum system, also known as the reverse effect (Back-action). In the condition of homodyne measurement, the noise produced by measurement output for zero error measurement is a one-dimensional Wiener process and it satisfies $E(dW) = 0, E[(dW)^2] = dt$. Based on the continuous weak measurement principles of the quantum system, measurement process contains the system evolution, so the continuous weak measurement operator

$M_0(\Delta t)$ contains the system total Hamiltonian $H(t)$. The evolution operators of the system by considering both system random noise and measurement efficiency are:

$$\begin{aligned} a_0(\Delta t) &= m_0(\Delta t) + \sqrt{\eta} L \cdot dW \\ a_1(\Delta t) &= m_1(\Delta t) + \sqrt{\eta} L \cdot dW \end{aligned} \tag{15}$$

where $\Delta t$ represents the very short time interval required for the weak measurement, $L \cdot dW$ denotes the noise caused by the continuous weak measurements, $\eta$ is the measurement efficiency which satisfies $0 < \eta \leq 1$, $dW$ is Gaussian white noise and $W(t)$ is a Weiner process with zero mean $E[W(t)] = 0$ and unit variance $E[(W(t))^2] = \delta$. Explicitly, the evolution operators of the $N$-qubit system are:

$$\begin{aligned} A_0(\Delta t) &= \underbrace{a_0(\Delta t) \otimes \ldots \otimes a_0(\Delta t) \otimes a_0(\Delta t)}_{N} \\ A_1(\Delta t) &= \underbrace{a_0(\Delta t) \otimes \ldots \otimes a_0(\Delta t) \otimes a_1(\Delta t)}_{N} \\ &\vdots \\ A_{2^N-1}(\Delta t) &= \underbrace{a_0(\Delta t) \otimes \ldots \otimes a_1(\Delta t) \otimes a_1(\Delta t)}_{N} \end{aligned} \tag{16}$$

The discrete-time dynamic evolution equation of the stochastic $N$-qubit open quantum system $S$ can be written by setting $t = k \times \Delta t$ as:

$$\rho(k+1) = A_0 \rho(k) A_0^\dagger + A_1 \rho(k) A_1^\dagger + \ldots + A_{2^N-1} \rho(k) A_{2^N-1}^\dagger \tag{17}$$

where $k$ is the sampling times in which we apply the continuous measurement and estimation.

Our objective is to estimate the state from continuous measurement records and dynamic of the system. The continuous weak measurement in Schrodinger picture is equivalent to the measurement of a constant state $\rho(0)$ with a continuously evolving measurement operator $M(t)$ in Heisenberg picture, by ignoring the noise and diffusion [26]. Hence, we transform system of Schrodinger picture in Eq. 14 to that of Heisenberg picture, where the measurement operator evolves continuously over time and the quantum state keeps constant. Note, this is not same as the standard Heisenberg picture, because we omit the decoherence during the dynamical evolution [25]. The evolution equation of the measurement operator $M(t)$ in Heisenberg picture is:

$$\dot{M}(t) = \frac{i}{\hbar}[H(t), M(t)] - \frac{1}{2}\left(L^\dagger L M(t) + M(t) L^\dagger L\right) + L^\dagger M(t) L \tag{18}$$

Therefore, the corresponding discrete-time evolution equation of continuous weak measurement operators for $N$-qubit can be written as:

$$M(k+1) = {M_0}^\dagger M(k) M_0 + {M_1}^\dagger M(k) M_1 + \ldots + {M_{2^N-1}}^\dagger M(k) M_{2^N-1} \tag{19}$$

One needs to set the amount of the initial measurement operator $M(0)$, and calculate the rest of the measurement operators by recursive Eq. 19. We study the effect of initial measurement operator $M(0)$ on the performance of our estimation later.

### 2.3. OQSE estimator

As we discussed in the introduction, to reconstruct the state, we need to solve Eq. 3. Here we propose an OQSE estimator which combines the non-negative least squares estimator of minimizing the 2-norm with the positive definite constraints of density matrix:

$$\begin{aligned} &\arg\min \|A \cdot vec(\hat{\rho}) - y\|_2 \\ &\text{s.t.} \quad \hat{\rho} \geq 0, \operatorname{tr}(\hat{\rho}) = 1 \end{aligned} \tag{20}$$

The vector $y$ and matrix $A$ can be expressed according to the current measurement configurations as:

$$y(l) = (\langle M(1)\rangle, \langle M(2)\rangle, \cdots, \langle M(l)\rangle)^T, l = 1, 2, ..., k \tag{21}$$

and

$$A(l) = \begin{pmatrix} vec(M(1))^T & vec(M(2))^T & \cdots & vec(M(l))^T \end{pmatrix}, l = 1, 2, ..., k \tag{22}$$

where the sampling matrix $A$ is the matrix form of all the sampled measurement operators in the $l$-th measurement as $M(l)$, $l = 1, 2, ..., k$, calculated by Eq. 19, with $k$ as the sampling times; The sampling vector $y$ is the vector form of the corresponding observation values $\langle M(l)\rangle$.

We can estimate the quantum state on-line, with a small number of time-evolving measurement operators $\langle M(l)\rangle$, $l = 1, 2, ..., k$ and corresponding measured records $y(l)$, $l = 1, 2, ..., k$ by solving the optimization problem Eq. 20 with an appropriate algorithm. To solve Eq. 20 we used CVX, a package for specifying and solving convex programs [39, 40].

The number of measurements $m$ is increasing as the sampling times increases, which makes the estimation process becomes time consuming. For instance at sampling times $k = 100$, we have 100 measurement operators Eq. 22 and corresponding records Eq. 21 which are used in the estimator. The estimator needs to estimate density matrix parameters, which are $d^2$ elements of density matrix in a $d$-dimensional Hilbert space. When the number of measurement outcomes are equal to $d^2$ the measurement set is known as informationally-complete, and if it's less than the number of elements, the measurement set is named as informationally-incomplete set. The measurement rate is defined as:

$$\beta = \frac{m}{d^2} \tag{23}$$

where $m$ is the number of measurements, and $d$ is the dimension of density matrix. Hence, for each state estimation we choose the last $m$ number of measurements and discard the others. The measurement rate is proportional to the number of measurements and when $\beta = 1$ the measurement set is informationally-complete set.

To study the performance of our state estimation scheme, we use fidelity and trace distance between actual state and estimated state as

$$F = Tr\sqrt{\hat{\rho}(t)^{1/2}\rho(t)\hat{\rho}(t)^{1/2}} \text{ and } Td = \frac{1}{2}tr\left(|\rho(t) - \hat{\rho}(t)|\right) \tag{24}$$

where $\hat{\rho}(t)$ is the estimated state and $\rho(t)$ the actual state of the system at time $t$. Generally, the trace distance $Td \in [0,1]$ is a measure of how much two states are close and fidelity $F \in [0,1]$ measures how much two states overlap each other. A trace distance of 0 (fidelity of 1) means the states are identical, whereas the trace distance of 1 (fidelity of 0) means the states are orthogonal.

## 3. Numerical experiments evaluation

To show the accuracy of the proposed estimation method, we perform numerical experiments. We study the effects of external control field, measurement rate and number of qubits on the performance of the OQSE by numerical simulations. In our numerical experiments, the Lindblad operator $L$ in Eq. 12 is chosen from the Stokes measurements set as:

$$B_0 = |H\rangle\langle H| + |V\rangle\langle V|,\ B_1 = |H\rangle\langle H|,\ B_2 = |D\rangle\langle D|,\ B_3 = |R\rangle\langle R| \tag{25}$$

where $|H\rangle \equiv |0\rangle = \begin{pmatrix} 1 \\ 0 \end{pmatrix}$ is horizontal polarization, $|V\rangle \equiv |1\rangle = \begin{pmatrix} 0 \\ 1 \end{pmatrix}$ is vertical polarization, $|D\rangle \equiv (|H\rangle + |V\rangle) \big/ \sqrt{2}$ is diagonal polarization, and $|R\rangle \equiv (|H\rangle + i|V\rangle) \big/ \sqrt{2}$ is right-circular polarization.

The initial state of each qubit is $\rho(0) = [\ 3/4 \quad -\sqrt{3}\big/4; \quad -\sqrt{3}\big/4 \quad 1/4\ ]$, hence, the initial state of $N$-qubit system is $\rho^N(0) = \underbrace{\rho(0) \otimes \cdots \otimes \rho(0)}_{N}$. The strength of the measurement is set as $\xi = 0.5$, the interval between two adjacent moments as $\Delta t = 0.1$, the measurement efficiency as $\eta = 0.5$, and the noise $dW$ is random generated Gauss white noise with variance being 0.02. The Hamiltonian of $\rho(t)$ is $H = H_0 + u_c H_c$ where $H_0 = \sigma_z$ is the free Hamiltonian of the system and $u_c H_c$ is the control Hamiltonian; $\sigma_x = \begin{bmatrix} 0 & 1 \\ 1 & 0 \end{bmatrix}$, $\sigma_y = \begin{bmatrix} 0 & -i \\ i & 0 \end{bmatrix}$ and $\sigma_z = \begin{bmatrix} 1 & 0 \\ 0 & -1 \end{bmatrix}$ are the Pauli operators.

### *3.1. The requirement of external control field to gain high fidelity*

As a first set of experiments, we compare the performance of the proposed OQSE for two-qubit initial state $\rho^2(0)$, with and without external control field. External control field appears in Hamiltonian of the system as $H = H_0 + u_x H_x$. When $u_x = 0$ ($u_x = 1$) the Hamiltonian is without (with) external control field, respectively. In the experiment, the measurement rate is set as $\beta = 1$, which is 16 number of measurements for two-qubit system. The definition of measurement rate $\beta$ can be found in Method Section.

As Fig. 1 depicted the fidelity of estimation is higher with external control field. By adding external control field, the amount of fidelity improves for different amounts of the Lindblad operator $L$ and initial measurement operator $M(0)$.

Now, we intend to find the reason of increase in the amount of fidelity by adding external control field. So we explain the relation between Hamiltonian of the system, Lindblad operator and the measurement operator $m_0(\Delta t)$. As we can see from Eq. 12,

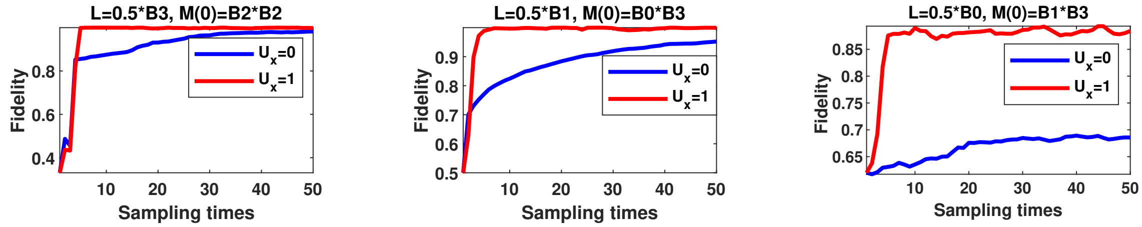


(a) (b) (c)

Figure 1: Fidelity between estimated state and actual state with and without external control field, for different amounts of Lindblad and initial measurement operator. The blue curve is the fidelity without external control, where $H = H_0 = \sigma_z$ , and the red curve is the fidelity with external control field, where $H = H_0 + u_x H_x$, $H_0 = \sigma_z$ is the free Hamiltonian of the system, $u_x H_x$ is the control Hamiltonian where $u_x = 1$.

the Hamiltonian of the system has effects on the amount of $m_0(\Delta t)$ for one-qubit and consequently on $M_j(\Delta t)$ in Eq. 13 for $N$-qubit. While Hamiltonian is without external control, $H = \sigma_z$, the amount of $m_0(\Delta t)$ for all Lindblad operators, is in the $x - z$ plane of the Bloch sphere and does not have y-component ( for $L = 0.5 * B_3$ the y-component is so small 0.01 according to Table 1). Hence, the estimated states are in the $x - z$ plane and are not close to the actual states of the system. However, by adding external control field as $H = \sigma_z + \sigma_x$, the measurement operator $m_0(\Delta t)$ has y-component for all Lindblad operators and can be in any plane of the Bloch sphere, as shown in Table 1. Therefore, the estimated states become closer to the actual states of the system, which can be in any plane of the Bloch sphere.

Table 1: The amount of y-component of measurement operator $m_0$ with and without external control for different Lindblad operators.

| Lindblad operator | $H = \sigma_z$ | $H = \sigma_z + \sigma_x$ |
|---|---|---|
| | y-component of $m_0(\Delta t)$ | y-component of $m_0(\Delta t)$ |
| $L = 0.5B_0$ | 0 | -0.2 |
| $L = 0.5B_1$ | 0 | -0.2 |
| $L = 0.5B_2$ | 0 | -0.2 |
| $L = 0.5B_3$ | 0.0125 | -0.1875 |

### *3.2. The effects of measurement rate on the performance of OQSE*

In order to find the behavior of our estimation method by changing the number of measurements, we do the simulation for initial two-qubit state $\rho^2(0)$ with different measurement rates. The definition of measurement rate $\beta$ can be found in Method Section. In Fig. 2 the behavior of fidelity for different measurement rates $\beta = 0.2, 0.3, 0.5, 1$ is given. The Hamiltonian is set as $H = \sigma_z + \sigma_x$, the Lindblad operator as $L = 0.5B_3$ and the initial measurement operator as $M(0) = B_2 \otimes B_2$.

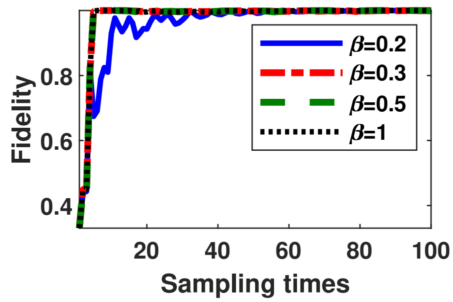


Figure 2: Fidelity between estimated state and actual state of two-qubit state $\rho^2(0)$ for different measurement rates.

From Fig. 2, we can see that the higher the measurement rate becomes, the higher fidelity gains. However, even with measurement rate $\beta = 0.3$, our estimation method gains high fidelity. By higher measurement rates the increase in the amount of fidelity is not much. According to Eq. 23, for the measurement rate $\beta = 0.2$, the number of measurements is $m = 3$; thus, after sampling times $k = 3$, only the last three measurement operators and corresponding results are using in the optimization algorithm. That is why we see a drop in the amount of fidelity after sampling times $k = 3$ for $\beta = 0.2$. However, As the sampling times increases, the amount of fidelity for all different measurement rates becomes closer, which is close to complete fidelity 100%. Table 2 is the specific amounts of fidelity at different sampling times for different measurement rates.

Table 2: Fidelity for two-qubit initial states $\rho^2(0)$ at different sampling times for different measurement rates.

| Sampling times / Measurement rate | $k = 3$ | $k = 5$ | $k = 10$ | $k = 50$ | $k = 100$ |
|---|---|---|---|---|---|
| $\beta = 0.2$ | 0.443 | 0.6741 | 0.9299 | 0.9955 | 0.9988 |
| $\beta = 0.3$ | 0.4499 | 0.9981 | 0.9999 | 0.9989 | 0.9998 |
| $\beta = 0.5$ | 0.4367 | 0.9984 | 0.9999 | 0.9983 | 0.999 |
| $\beta = 1$ | 0.4474 | 0.9999 | 0.9979 | 0.9971 | 0.9999 |

As Table 2 shows, with $\beta = 0.3$ or higher measurement rates, the amount of fidelity is more than 99% after sampling times 5. Hence, to gain high fidelity at low sampling times, measurement rate $\beta = 0.3$ is enough.

### *3.3. Density matrix of the system during sampling times*

Here, we study the behavior of the state during the sampling times. Fig. 3 shows the density matrix of the two-qubit state $\rho^2(0)$ at sampling times 10, 50 and 100. Also the behavior of fidelity and trace distance between the actual state and the estimated state during sampling times is given. The experimental simulation is done by setting variables as follow: $M(0) = B_2 \otimes B_2$, $L = 0.5B_3$, and the total sampling times of the continuous weak measurement is 100 in the experiments. The Hamiltonian of $\rho(t)$ is $H = \sigma_z + \sigma_x$ which has the external control field. The measurement rate is set as $\beta = 0.3$. The density matrix of the system at sampling times 100 is

$$\rho_{100} = \begin{pmatrix} 0.1393 & 0.0176+0.007i & 0.0176+0.007i & 0.0019+0.0018i \\ 0.0176-0.007i & 0.2339 & 0.0026 & 0.0296+0.0118i \\ 0.0176-0.007i & 0.0026 & 0.2339 & 0.0296+0.0118i \\ 0.0019-0.0018i & 0.0296-0.0118i & 0.0296-0.0118i & 0.3929 \end{pmatrix}.$$

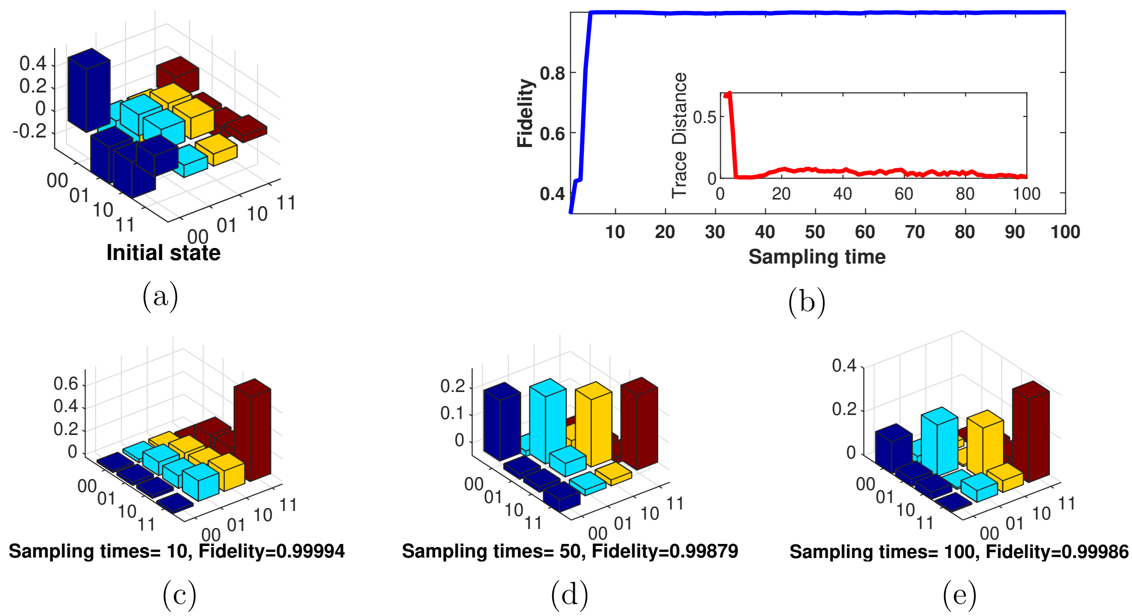


Figure 3: Density matrix of the two-qubit state, fidelity and trace distance between actual state and estimated state at different sampling times.

As Fig. 3 depicted, the fidelity between actual state and estimated state is higher than 99% after sampling times 5. We note that, in the first sampling times, the number of measurements and corresponding records are not enough for the estimator to reconstruct the state of the system accurately. However, after enough sampling times, the fidelity of the OQSE method reaches the highest amount, which is complete fidelity 100%.

The diagonal elements of the density matrix changes during the evolution of the system and continuous measurements. Fig. 4 shows the behavior of the diagonal elements of $\rho^2(0)$ over sampling times. Since the actual and estimated state are equal, we plot the elements of one of the density matrices. After sampling times 100 the specific amounts of the diagonal elements of the density matrix are: $\rho_{11} = 0.1393$, $\rho_{22} = 0.2339$, $\rho_{33} = 0.2339$ and $\rho_{44} = 0.3929$.

For three-qubit system, eight measurement operators are needed. The initial

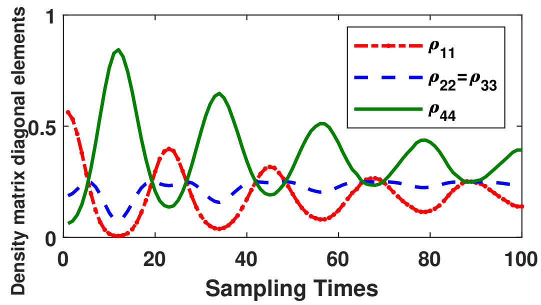


Figure 4: Diagonal elements of density matrix $\rho^2(0)$ over sampling times.

density matrix of the three-qubit system is $\rho^3(0)$. The results of experimental simulation are shown in Fig. 5. The initial measurement operator is set as $M(0) = B_2 \otimes B_2 \otimes B_2$ and the measurement rate is $\beta = 0.3$.

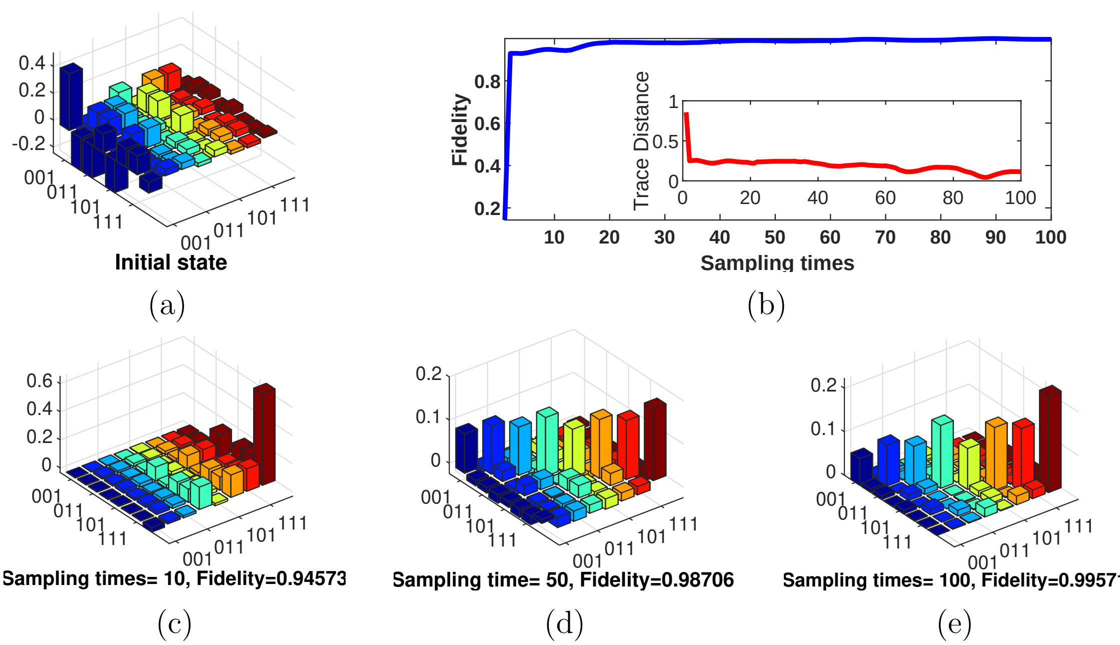


Figure 5: Density matrix of the three-qubit system and fidelity between actual state and estimated state at different sampling times.

As one can see from Fig. 3 and Fig. 5, the state of the system changes during the sampling times because of the evolution of the system. According to the amount of fidelity, the OQSE estimates the state of the system accurately, in real time as the state changes.

### *3.4. N-qubit OQSE with minimum measurement rate*

The question here arises as, what is the minimum measurement rate (number of measurements) for each number of qubits to gain high fidelity. We note that as the sampling times proceed, the number of measurement operators and corresponding records, used in optimization algorithm, increase. For instance, at sampling times 50, optimization algorithm is using 50 measurement operators and corresponding records. To find the minimum measurement rate for each number of qubits to gain high fidelity, we do the estimation process without dropping any measurement records. In this case, sampling times are equal to the number of measurements. In Table 3 we give the first time that the amount of fidelity reaches 98% and 99% for each number of qubits, also the corresponding measurement rates according to Eq.21 is given.

Table 3: The sampling times and corresponding measurement rate, where the amount of fidelity reaches 98% and 99% for different number of qubits.

| Number of qubits | Reaching fidelity 98% | | Reaching fidelity 99% | |
|---|---|---|---|---|
| | Sampling times | Corresponding measurement rate | Sampling times | Corresponding measurement rate |
| 2-qubit | 5 | 0.31 | 5 | 0.31 |
| 3-qubit | 20 | 0.31 | 44 | 0.68 |
| 4-qubit | 38 | 0.14 | 44 | 0.17 |
| 5-qubit | 39 | 0.03 | 47 | 0.04 |

As Table 3 shows, for higher number of qubits, the amount of fidelity reaches 99% in longer sampling times. However, the measurement rate is smaller. For instance, 5-qubit density matrix has 1024 elements, which means the estimator must estimate 1024 elements. As we show in Table 3, OQSE gains 99% fidelity by 47 measurement operators and corresponding records which is measurement rate 0.04.

To better demonstrate the behavior of the performance of the proposed estimation method for different number of qubits, the fidelity for different number of qubits $N = 2, 3, 4$ and 5 is given in Fig. 6. The measurement rate for each number of qubits is set according to Table 3. For 2, 3, 4 and 5-qubit the measurement rate is set as 0.31, 0.68, 0.17 and 0.04, respectively.

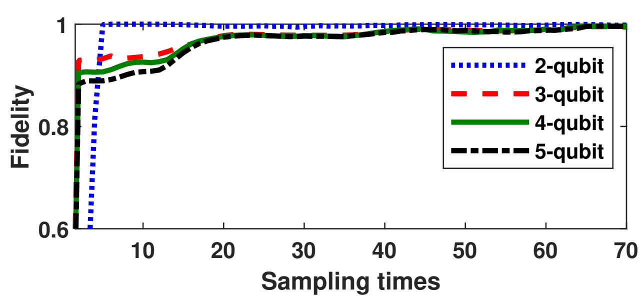


Figure 6: Fidelity for different number of qubits $N$= 2, 3, 4 and 5.

As one can see from Fig. 6, by increasing the number of qubits, since the size of the density matrix increases and the estimator needs to estimate more elements, the complete fidelity gains at longer sampling times. However, as the number of qubits increases (consequently the size of the estimated density matrix increases), OQSE estimates the state with fidelity 99% by smaller measurement rate.

## Discussion

The proposed OQSE estimates the $N$-qubit quantum states in real time with high fidelity and small number of measurements. We study the OQSE with continuous weak measurements and compressed sensing. The indirect weak measurements are used and the time dependent measurement operators in presence of dynamic evolution of the system are derived. The dynamic of the system is presented by stochastic master equation in Schrodinger picture; and the continuous weak measurements in presence of dynamic evolution of the system are given by transforming the system of Schrodinger picture to that of Heisenberg picture. We verified the proposed OQSE by simulation experiments and used least square algorithm to calculate the results.

The simulation results show that in order to obtain high fidelity for estimation, one needs to add external control field to Hamiltonian of the system. By adding the external control field, the estimated states are located in the same plane of the actual states which makes the OQSE more accurate. We study the behavior of the density matrix of the system during the continuous weak measurement and on-line estimation for 2 and 3-qubits. The results of study show that the state becomes mixed during the sampling times of the estimation. In addition, the minimum measurement rate to gain high fidelity is given for $N$-qubit system. We show that the proposed OQSE can gain fidelity higher than 99% with small number of measurements.

## 4. Acknowledgments

This work was supported by the National Natural Science Foundations of China under Grant No. 61573330 and 61720106009.

## 5. References

[1] Häffner H,.. 2005 *Nature* **438** 643–646
[2] O'Brien J L, Pryde G J, White A G, Ralph T C and Branning D 2003 *Nature* **426** 264
[3] D'Ariano G M, Paris M G A and Sacchi M F 2003 *Adv. Imaging Electron Phys.* **128** 206–309
[4] Sugiyama T, Turner P S and Murao M 2011 *Phys. Rev. A* **83** 12105
[5] Burgarth D, Giovannetti V, Kato AN and Yuasa K 2015 *New J. Phys.* **17** 113055
[6] de Burgh M D, Langford N K, Doherty A C and Gilchrist A 2008 *Phys. Rev. A* **78** 52122
[7] Gross D, Liu Y K, Flammia S T, Becker S and Eisert J 2010 *Phys. Rev. Lett.* **105** 1–4
[8] Shojaee E, Jackson C S, Riofrio C A, Kalev A and Deutsch I H 2018 *Phys. Rev. Lett.* **121** 130404
[9] Six P, Campagne-Ibarcq P, Dotsenko I, Sarlette A, Huard B and Rouchon P 2016 *Phys. Rev. A* **93**, 12109
[10] Riofrío C A, Jessen P S and Deutsch I H 2011 *J. Phys. B At. Mol. Opt. Phys.* **44**, 154007
[11] Kim Y, Kim YS, Lee SY, Han SW, Moon S, Kim YH and Cho YW 2018 *Nat. Commun.* **9(1)** 192
[12] Bassa H, Goyal SK, Choudhary SK, Uys H, Diósi L and Konrad T 2015 *Phys. Rev. A* **92**, 32102
[13] Blume-Kohout R 2010 *New J. Phys.* **12**, 43034
[14] Hradil Z, Řeháček J, Fiurášek J and Ježek M 2004 *Quantum State Estimation* springer 59–112
[15] Bolduc E, Knee G C, Gauger E M and Leach J 2017 *npj Quantum Inf.* doi:10.1038/s41534-017-0043-1.

[16] Home J P, Hanneke D, Jost JD, Amini JM, Leibfried D and Wineland DJ 2009 *Science* **325**, no. 5945, 1227-1230

[17] Barreiro J T, Müller M, Schindler P, Nigg D, Monz T, Chwalla M, Hennrich M, Roos C F, Zoller P and Blatt R 2011 *Nature* **470**, 486

[18] Harraz S, Yang J, Li K and Cong S 2016 *Optim. Control Appl. Methods* **38(5)**, 744-753

[19] Harraz S, Cong S and Shuang F 2018 *IEEE 7th Data Driven Control Learn. Syst. Conf.* 302–307

[20] Oreshkov O and Brun T 2005 *Phys. Rev. Lett.* **95**, 1–4

[21] Smith A, Riofrío CA, Anderson BE, Sosa-Martinez H, Deutsch IH and Jessen PS 2013 *Phys. Rev. A - At. Mol. Opt. Phys.* **87**, 1–5

[22] Yang J, Cong S and Kuang S 2018 *Proceedings of the International MultiConference of Engineers and Computer Scientists 2018*, Vol **II**

[23] Geremia J M, JK Stockton and H Mabuchi 2004 *Science* **304**, 270

[24] Mølmer K and Madsen L B 2004 *Phys. Rev. A* **70**, 52102

[25] Riofrío C A, Jessen P S and Deutsch I H 2011 *J. Phys. B At. Mol. Opt. Phys.* **44**, 1–19

[26] Smith G A, Silberfarb A, Deutsch I H and Jessen P S 2006 *Phys. Rev. Lett.* **97**, 1–4

[27] Kalev A and Hen I 2015 *New J. Phys.* **17**

[28] Butucea C, Guţe M and Kypraios T 2015 *New J. Phys.* **17**

[29] Cong S, Tang Y, Harraz S, K Li and Yang J 2018 *SCIENCE CHINA Information Sciences* doi: 10.1007/s11432-018-9793-2

[30] Yang J, Cong S and Shuang F 2018 *International Conference on Engineering, Science and Applications (ICESA 2018), Tokyo, Japan,* 63–76

[31] Candès E J, Romberg J and Tao T 2006 *IEEE Trans. Inf. theory,* **52**, 489–509

[32] Kyrillidis A, Kalev A, Park D, Bhojanapalli S, Caramanis C and Sanghavi S 2018 *npj Quantum Inf.* **4**, 36

[33] Kalev A, Kosut R L and Deutsch I H 2015 *Nat. Publ. Gr.* doi:10.1038/npjqi.2015.18

[34] Donoho D L 2006 *IEEE Trans. Inf. theory.* **52** 1289–1306

[35] Candes E J, Romberg J and Tao T 2006 *IEEE Trans. Inf. theory.* **52** 489-509

[36] Candes E J and Tao T 2006 *IEEE Trans. Inf. theory.* **52** 5406–5425

[37] Flammia S T, Gross D, Liu Y K and Eisert J *New J. Phys.* **14**

[38] Cong S 2014 Control of Quantum Systems: Theory and Methods. *John Wiley & Sons*

[39] Grant M C and Boyd S P 2008 *Springer* 95–110

[40] Grant M, Boyd S and Ye Y 2008 CVX: Matlab software for disciplined convex programming.